AMP-activated protein kinase activation and NADPH oxidase inhibition by inorganic nitrate and nitrite prevent liver steatosis

Isabel Cordero-Herrera[a], Mikael Kozyra[a], Zhengbing Zhuge[a], Sarah McCann Haworth[a], Chiara Moretti[a], Maria Peleli[a], Mayara Caldeira-Dias[a], Arghavan Jahandideh[a], Han Huirong[a], Josiane de Campos Cruz[a], Andrei L. Kleschyov[a,b], Marcelo F. Montenegro[a], Magnus Ingelman-Sundberg[a], Eddie Weitzberg[a,c], Jon O. Lundberg[a,1,2], and Mattias Carlstrom[a,1,2]

[a]Department of Physiology and Pharmacology, Karolinska Institutet, 17177 Stockholm, Sweden; [b]Laboratory of Biophysics, Freiberg Instruments Ltd., 09599 Freiberg, Germany; and [c]Department of Perioperative Medicine and Intensive Care, Karolinska University Hospital, 17176 Stockholm, Sweden

Edited by Louis J. Ignarro, University of California, Los Angeles School of Medicine, Beverly Hills, CA, and approved November 16, 2018 (received for review June 4, 2018)

Advanced age and unhealthy dietary habits contribute to the increasing incidence of obesity and type 2 diabetes. These metabolic disorders, which are often accompanied by oxidative stress and compromised nitric oxide (NO) signaling, increase the risk of adverse cardiovascular complications and development of fatty liver disease. Here, we investigated the therapeutic effects of dietary nitrate, which is found in high levels in green leafy vegetables, on liver steatosis associated with metabolic syndrome. Dietary nitrate fuels a nitrate–nitrite–NO signaling pathway, which prevented many features of metabolic syndrome and liver steatosis that developed in mice fed a high-fat diet, with or without combination with an inhibitor of NOS (L-NAME). These favorable effects of nitrate were absent in germ-free mice, demonstrating the central importance of host microbiota in bioactivation of nitrate. In a human liver cell line (HepG2) and in a validated hepatic 3D model with primary human hepatocyte spheroids, nitrite treatment reduced the degree of metabolically induced steatosis (i.e., high glucose, insulin, and free fatty acids), as well as drug-induced steatosis (i.e., amiodarone). Mechanistically, the salutary metabolic effects of nitrate and nitrite can be ascribed to nitrite-derived formation of NO species and activation of soluble guanylyl cyclase, where xanthine oxidoreductase is proposed to mediate the reduction of nitrite. Boosting this nitrate–nitrite–NO pathway results in attenuation of NADPH oxidase-derived oxidative stress and stimulation of AMP-activated protein kinase and downstream signaling pathways regulating lipogenesis, fatty acid oxidation, and glucose homeostasis. These findings may have implications for novel nutrition-based preventive and therapeutic strategies against liver steatosis associated with metabolic dysfunction.

nitrate | nitrite | nitric oxide | steatosis | microbiota

Occurrence of metabolic syndrome has increased dramatically worldwide, and, consequently, the prevalence of type 2 diabetes (T2D) is soon reaching 10%. Reports from the World Health Organization (WHO) project the number of adults living with T2D in 2040 to be >650 million globally, with more than 20% of the US population affected. Increased prevalence of T2D is largely reflected by being overweight or obesity in the society, and associated morbidities and mortalities are immense.

Nonalcoholic fatty liver disease (NAFLD) is the most common liver disease in the world and is strongly associated with being overweight, obesity, and the metabolic syndrome (1). In the United States, 25% of the population is affected, and almost half of these have received a diagnosis of T2D. NAFLD can be reversed by weight loss and exercise but can also progress to nonalcoholic steatohepatitis and further to liver fibrosis and cirrhosis. Attempts have been made to identify a common underlying molecular mechanism that can explain the various features of the metabolic syndrome and associated complications (2, 3). One such candidate mechanism, linking cardiometabolic disease in humans, is impaired nitric oxide (NO) bioavailability and signaling (4, 5). NO synthase (NOS) is generally thought to be the source of endogenously produced NO, a pleiotropic signaling molecule involved in cardiovascular and metabolic regulation. Endothelial NOS (eNOS) gene polymorphisms have been associated with metabolic syndrome and T2D in humans (6–8), and eNOS-deficient mice display hypertension, dyslipidemia, insulin resistance, and accumulation of visceral adipose tissue, which are the key features of metabolic syndrome (9–11).

In addition to the classical L-arginine–dependent NOS system, an alternative route for NO generation has been identified, wherein the inorganic anions nitrate and nitrite are serially reduced to NO and other bioactive nitrogen oxide intermediates (12). Bioactivation of nitrate involves its selective accumulation in the salivary glands and active secretion into the oral cavity, followed by reduction to the more reactive nitrite anion. This nitrite formation is believed to involve oral commensal nitrate-reducing

Significance

Liver steatosis, or fatty liver, is the most common liver disease in the world, affecting up to 25% of all Americans. There is currently no approved drug available for this condition, which may progress to serious disease, including steatohepatitis, fibrosis, and cirrhosis. Here, we show in rodent and human models of metabolic syndrome that steatosis can be prevented by a simple dietary approach. Inorganic nitrate, present in green leafy vegetables, is converted in vivo to nitric oxide (NO) in a process involving symbiotic host bacteria. NO then induces key metabolic regulatory pathways to ultimately reduce oxidative stress and improve cardiometabolic functions. Clinical trials would be helpful to tell if dietary nitrate is useful in treatment and prevention of fatty liver disease.

Author contributions: A.L.K., M.F.M., M.I.-S., E.W., J.O.L., and M.C. designed research; I.C.-H., M.K., Z.Z., S.M.H., C.M., M.P., M.C.-D., A.J., H.H., J.C.C., A.L.K., M.F.M., and M.C. performed research; I.C.-H., M.K., C.M., A.L.K., M.F.M., M.I.-S., and M.C. contributed new reagents/analytic tools; I.C.-H., M.K., Z.Z., S.M.H., C.M., M.P., M.C.-D., A.J., H.H., J.C.C., A.L.K., M.F.M., M.I.-S., E.W., J.O.L., and M.C. analyzed data; and E.W., J.O.L., and M.C. wrote the paper.

Conflict of interest statement: J.O.L. and E.W. are coinventors on patent applications related to the therapeutic use of inorganic nitrate. M.I.-S. is cofounder of HepaPredict AB.

This article is a PNAS Direct Submission.

[1]J.O.L. and M.C. contributed equally to this work.

[2]To whom correspondence may be addressed. Email: jon.lundberg@ki.se or mattias.carlstrom@ki.se.

This article contains supporting information online at www.pnas.org/lookup/suppl/doi:10.1073/pnas.1809406115/-/DCSupplemental.

Published online December 17, 2018.

bacteria (13). Further metabolism of nitrite to form NO and other bioactive nitrogen oxides occurs systemically in blood and tissues and is catalyzed by a variety of proteins and enzymes, including deoxygenated hemoglobin (14) and xanthine oxidoreductase (XOR) (15). Accumulating evidence clearly shows that the nitrate–nitrite–NO pathway is involved in regulation of cardiometabolic functions in both healthy and disease states (12, 16, 17). Dietary supplementation with inorganic nitrate, to boost this alternative pathway of NO formation, has therapeutic effects in experimental models of metabolic syndrome and T2D (18–20), which, at least in part, may be linked to modulation of mitochondrial function (21), reduction of NADPH oxidase (NOX)-derived oxidative stress (18, 22, 23), and immune cell regulation (24, 25). Moreover, epidemiological dietary studies have shown that increased intake of vegetables which are rich in nitrate conveys antiobesity and antidiabetic effects and protects against development of cardiovascular disease and T2D (26–29).

Considering the important role of NO in regulation of metabolic functions, the aim of the present study was to investigate potential salutary effects of nitrate administration on the development or progression of liver steatosis associated with obesity and metabolic syndrome and to explore possible underlying mechanisms. Our results from the in vivo disease model in mice and in vitro studies using HepG2 cells and primary human hepatocyte spheroids indicate that stimulation of the nitrate–nitrite–NO pathway may attenuate the development of liver steatosis via mechanisms that involve activation of AMP-activated protein kinase (AMPK) signaling and reduction of NOX-derived oxidative stress.

Results

An overview of the experimental protocol is shown in *SI Appendix*, Fig. S1.

In Vivo Mouse Model (Part I).

Dietary nitrate alleviates features of metabolic syndrome. To see if the animals developed metabolic syndrome following chronic treatment with a high-fat diet (HFD) and a NOS inhibitor [Nω-Nitro-L-arginine methyl ester hydrochloride (L-NAME)], body weight and composition, glucose clearance, insulin sensitivity, blood pressure, and vascular reactivity were measured. Mice fed with an HFD significantly increased in body weight, fat mass, and percentage of fat, without changes in lean mass (Table 1). Similar abnormalities were observed in mice receiving nitrate supplementation (Table 1). HFD-treated mice also had increased fasting blood glucose levels, and these were significantly lower in the nitrate group (Table 1). In addition, an impaired glucose clearance was seen in mice fed an HFD, and this was prevented by nitrate (Fig. 1 *A* and *B*). HFD-treated mice developed insulin resistance, which was prevented by nitrate treatment (Fig. 1 *C* and *D*). HFD treatment was also linked with increased blood pressure (Fig. 1*E*) and impaired endothelium-dependent vasorelaxation to acetylcholine (Fig. 1*F*). The higher blood pressure was most likely mainly driven by the L-NAME treatment added to the HFD. Nitrate completely prevented the rise in blood pressure and significantly preserved endothelial function.

Table 1. Metabolic characteristics of mice treated with an HFD

Parameter	Control	HFD	HFD + nitrate
N	9	9	10
BW start, g	22.4 ± 0.4	21.8 ± 0.2	21.9 ± 0.5
BW end, g	25.0 ± 0.5*	26.7 ± 0.5*,#	27.6 ± 0.9*,#
Total lean mass, g	21.2 ± 0.6	20.1 ± 0.4	20.5 ± 0.4
Total fat, g	3.8 ± 0.1	6.5 ± 0.5#	6.6 ± 0.6#
Total fat/lean mass, %	18.1 ± 0.6	32.4 ± 2.9#	31.8 ± 2.8#
Abdominal fat/BW, %	14.8 ± 0.5	24.5 ± 2.2#	23.7 ± 1.8#
Fasting blood glucose, mM	7.2 ± 0.2	10.1 ± 0.4#	8.6 ± 0.1

BW, body weigh; *n*, number of mice per group.
*$P < 0.05$ vs. start (within group).
#$P < 0.05$ vs. control group.

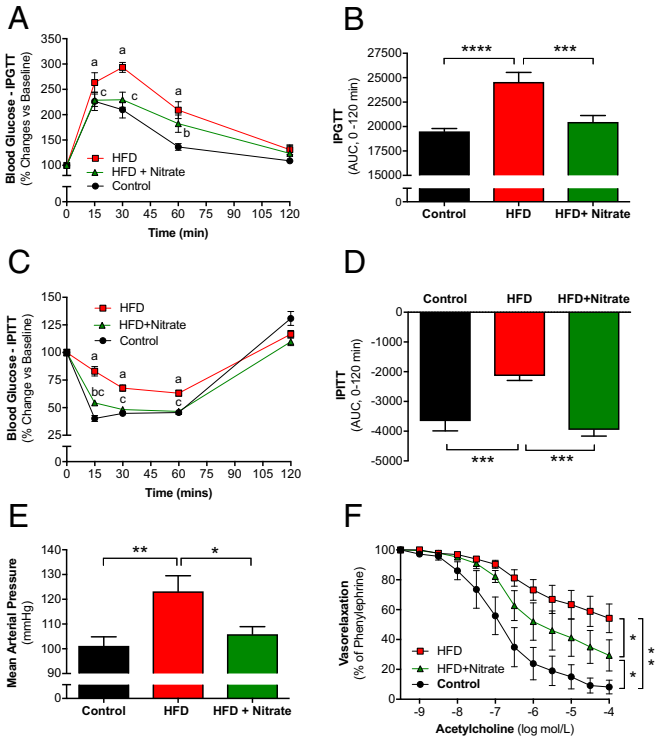

Fig. 1. Cardiovascular and metabolic phenotype. (*A*) After 5 wk of dietary treatment with an HFD in combination with the NOS inhibitor L-NAME, mice were subjected to an i.p. glucose tolerance test (IPGTT) (2 g/kg body weight), and time-course changes in glucose levels were measured. (*B*) Area under the curve (AUC) calculated from IPGTT data. (*C*) Intraperitoneal insulin tolerance tests (IPITTs) were performed after 6 wk of treatment (0.75 IU/kg body weight), and glucose levels were followed for 2 h. (*D*) Inverse AUC calculated from IPITT data. (*E*) Mean arterial blood pressure was recorded by the noninvasive tail monitoring system at week 6 of treatment. (*F*) At killing (i.e., 7 wk of treatment), fresh mesenteric arteries from the mice were isolated, and reactivity to increasing concentrations of acetylcholine was measured. Data are presented as the mean ± SEM. $n = 6$ to 10 mice per group. *, **, ***, **** denote $P < 0.05$, $P < 0.01$, $P < 0.001$, and $P < 0.0001$, respectively, between indicated groups. An "a" denotes $P < 0.05$ between Control vs. HFD, "b" denotes $P < 0.05$ between Control vs. HFD+Nitrate, and "c" denotes $P < 0.05$ between HFD vs. HFD+Nitrate. Tests were performed by two-way repeated measures (RM) ANOVA (*A*, *C*, and *F*) or one-way ANOVA followed by Holm–Sidak test (*B*, *E*, and *D*). IPGTT, i.p. glucose tolerance test; IPITT, i.p. insulin tolerance test; HFD, high-fat diet+L-NAME.

In a separate series, the effects of dietary nitrate in animals fed an HFD alone (without L-NAME) were tested. The cardiometabolic abnormalities that developed with the HFD were largely prevented also in this model (*SI Appendix*, Figs. S2 and S3).

Dietary nitrate restores nitrate, nitrite, and iron-nitrosylated hemoglobin levels in blood and dinitrosyl–iron complexes in liver. The model of metabolic syndrome used here utilizes an HFD in combination with an NOS inhibitor. Therefore, one would expect to see a decrease in plasma and tissue levels of nitrate and nitrite. Indeed, nitrate levels in plasma and liver from HFD mice were reduced, and, as expected, these were significantly increased by dietary nitrate (Fig. 2 *A*–*C*). Plasma nitrite was also reduced by the HFD and restored to control levels in the nitrate group. There were no differences in liver nitrite levels among the groups (Fig. 2*D*). EPR analysis of blood and liver samples directly demonstrated the restoration of compromised tissue NO levels by dietary nitrate. Thus, the treatment with HFD+L-NAME markedly decreased the blood iron-nitrosylated hemoglobin (Hb-NO) and liver dinitrosyl–iron complex (DNIC) levels; these were largely prevented by dietary nitrate (Fig. 2 *E* and *F*).

Nitrate prevents liver steatosis and attenuates NOX activity. Liver sections stained with Oil Red O demonstrated that HFD in the

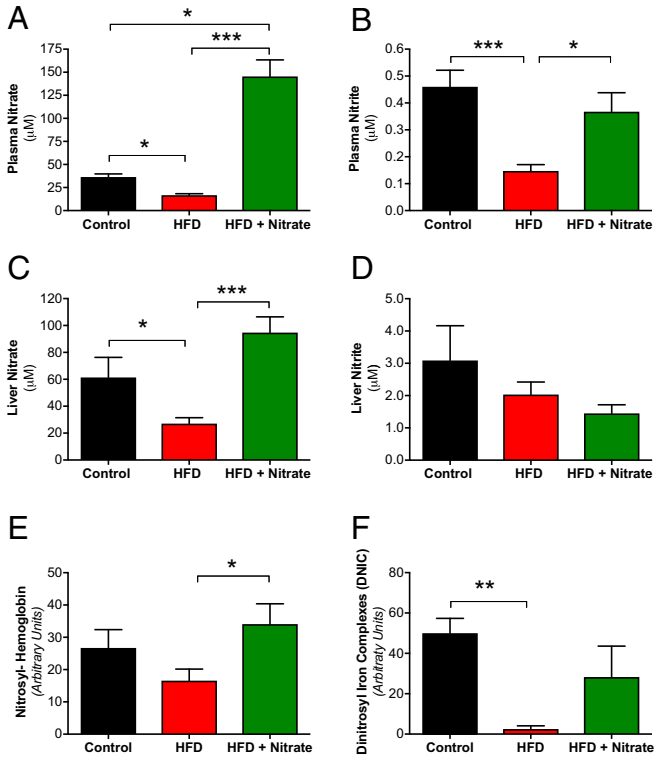

Fig. 2. Nitrate, nitrite, and iron-nitrosylated species levels in blood and liver. In tissues obtained after 7 wk of dietary treatment with an HFD in combination with the NOS inhibitor L-NAME, (*A*) plasma nitrate, (*B*) plasma nitrite, (*C*) liver nitrate, (*D*) liver nitrite, (*E*) blood iron-nitrosylated-hemoglobin, and (*F*) liver dinitrosyl iron complexes (DNICs) were measured for the three animal groups. Data are presented as the mean ± SEM. $n = 6$ to 9 per group. *, **, and *** denote $P < 0.05$, $P < 0.01$, and $P < 0.001$, respectively, between indicated groups tested by Kruskal–Wallis test and Dunn's test (*A*–*E*). HFD, high-fat diet+L-NAME.

presence of L-NAME led to increased lipid accumulation compared with the control group, and this was fully prevented by nitrate (Fig. 3 *A* and *B*). HFD also increased NOX-derived superoxide production in the liver (Fig. 3*C*), and this was prevented by nitrate. Moreover, there was a positive correlation between lipid accumulation and NOX activity (Fig. 3*F*). To examine how nitrate could modulate NOX activity, the levels of the NOX subunit p67phox and NOX2 (gp91phox) were measured by Western blot. HFD significantly increased p67phox levels (twofold increase). In line with the results above, nitrate prevented p67phox up-regulation (Fig. 3*D*). No changes in the expression of NOX2 were seen (Fig. 3*E*).

Host microbiota are necessary for dietary nitrate to prevent steatosis. Oral bacteria are believed to be central in bioactivation of dietary nitrate as they catalyze its reduction to the more reactive nitrite anion, a reaction that cannot be as effectively performed by mammalian enzymes (30). When germ-free mice were fed an HFD and L-NAME for the same duration as in conventional mice, they also developed liver steatosis. However, while nitrate prevented steatosis in conventional mice (Fig. 3 *A* and *B*), it was without effect in germ-free mice (Fig. 4), indicating the central involvement of commensal bacteria in bioactivation of nitrate to elicit protective nitric oxide signaling. Similarly, abnormal glucose tolerance, increased fat content, and cardiac hypertrophy in germ-free mice were also not improved by the nitrate treatment (*SI Appendix*, Table S1).

Nitrate prevents the AMPK inhibition induced by an HFD. AMPK is considered a central regulator of glucose and lipid metabolism in the liver and plays a key role in preventing lipid accumulation in hepatocytes. Akt is one of the downstream proteins of the insulin-signaling pathway, which is often disrupted in the metabolic syndrome and type 2 diabetes. Decreased phosphorylated levels of AMPK and Akt were observed in the livers of HFD-fed mice (Fig. 5). Livers from nitrate-supplemented mice displayed phospho-AMPK (p-AMPK)/AMPK ratios similar to control levels while the phospho-Akt (p-Akt)/Akt ratios were not significantly affected. Thus, the preventive effect of nitrate on steatosis likely involves preserved AMPK signaling.

Nitrate modulates genes and proteins involved in lipid metabolism. With indications of the AMPK signaling pathway being involved in the salutary effects of nitrate, we next analyzed some of its key downstream target proteins involved in cholesterol and fatty acid synthesis, fatty acid oxidation, and mitochondrial biogenesis. Messenger RNA expression and protein levels of the lipogenic transcription factor sterol regulatory element-binding protein 1 (SREBP1c), acetyl-CoA carboxylase (ACC), and peroxisome proliferator-activated receptor γ coactivator 1 (PGC1α), as well

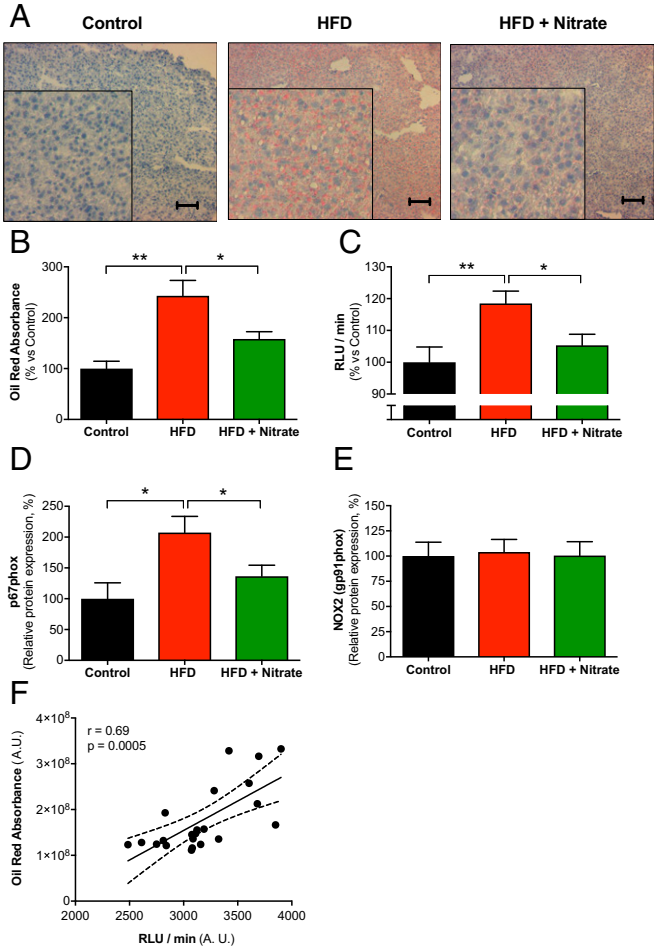

Fig. 3. Oil-Red O staining and NADPH oxidase activity in liver. (*A*) Representative images of liver sections from the three mice groups at the moment of killing stained with Oil Red O to visualize neutral lipids and Mayer's hematoxylin to visualize the cell nuclei and tissue morphology. (Scale bars: 1 μm.) *Insets* show four times magnified details of the images to highlight the lipid-staining morphology. (*B*) Quantification of neutral lipids in liver sections using ImageJ software. (*C*) NADPH oxidase-derived superoxide and hydrogen peroxide production was measured by Amplex red and expressed as relative light units (RLUs), in the liver of the three groups of mice at killing. (*D* and *E*) p67phox and NOX2 (gp91phox) protein levels in the liver were determined by Western blot. Densitometric quantification is presented as p67phox/vinculin and NOX2/vinculin. (*F*) Correlation between Oil Red O staining and NADPH oxidase activity in the liver. Data are presented as the mean ± SEM. $n = 5$ to 9 per group. * and ** denote $P < 0.05$ and $P < 0.01$, respectively, between indicated groups, tested by Kruskal–Wallis test and Dunn's test (*B*, *C*, and *E*) or Pearson correlation test (*D*). HFD, high-fat diet+L-NAME.

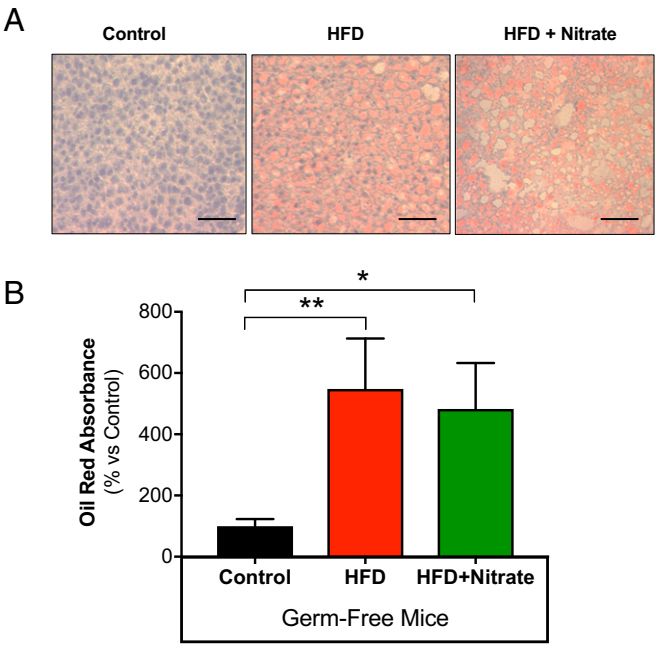

Fig. 4. Oil-Red O staining in livers of germ-free mice. (*A*) Representative images of liver sections from the three groups of germ-free mice at killing, stained with Oil Red O to visualize neutral lipids and Mayer´s hematoxylin to visualize the cell nuclei and tissue morphology. (Scale bars: 5 μm.) (*B*) Quantification of neutral lipids in liver sections was done using ImageJ software. Data are presented as the mean ± SEM. $n = 5$ to 6 per group. * and ** denote $P < 0.05$ and $P < 0.01$, respectively, between indicated groups, tested by Kruskal–Wallis test and Dunn's test. HFD, high-fat diet+L-NAME.

as lipolytic medium chain acyl-CoA dehydrogenase (ACADM), were measured in the liver of the mice

Although not statistically significant, there was a tendency for increased SREBP1c mRNA levels by the HFD ($P = 0.08$) that was prevented by nitrate (Fig. 6*A*). SREBP1c protein levels were significantly increased by the HFD, and this was not observed in HFD mice with nitrate treatment (Fig. 6*B*). HFD significantly reduced mRNA and phosphorylated levels of ACC, and, again, this was prevented by dietary nitrate (Fig. 6 *C* and *D*). PGC1α mRNA levels were unchanged by HFD but increased with nitrate (Fig. 6*E*). HDF dramatically reduced PGC1α protein levels (Fig. 6*F*), which trended ($P = 0.08$) to be prevented by nitrate. Finally, there was a decrease in both mRNA and protein levels of the lipolytic ACADM by the HFD, and this was not observed in the nitrate group (Fig. 6 *G* and *H*).

All together, these results suggest that nitrite prevents HFD-induced lipogenesis and reduction in β-oxidation in the liver. This imbalance between de novo lipogenesis and lipid catabolism could explain the lipid accumulation in the liver of the HFD mice and how nitrate prevents it.

HepG2 Cells (Part II).

Nitrite prevents lipid accumulation and NOX-derived superoxide production in HepG2 cells. To more thoroughly study the mechanisms behind the observed effects of nitrate in vivo, we next established a model of steatosis in a human liver cell line. HepG2 cells were treated for 24 h with glucose, insulin, and free fatty acids (FFAs) to induce steatosis. This treatment significantly increased lipid accumulation in the cells (Fig. 7 *A* and *B*), demonstrating its usefulness as a steatosis model. Incubation with nitrite prevented lipid accumulation in these cells, as determined by Oil Red O staining. Incubation of cells with the steatosis mixture for a longer period of time (48 h) further increased NOX-derived superoxide generation. However, after 72-h treatment, the chemiluminescence signal decreased, and this can partly be explained by extensive cell death (*SI Appendix*, Fig. S4).

In agreement with the in vivo data, we observed increased NOX-derived superoxide generation during steatosis development (Fig. 7*C*), reflecting an increase in oxidative stress and an imbalance in redox status. This increase in NOX activity was largely prevented by nitrite (Fig. 7*C*).

To better establish a causal link between NOX-derived superoxide generation and development of steatosis, we incubated the cells also with the superoxide scavenger tempol, a NOX2/4 inhibitor (GLX481304), or a selective and potent NOX4 inhibitor (GLX7013114). Preincubation with tempol prevented both lipid accumulation and superoxide generation (Fig. 7 *D* and *E*), thus supporting a role of NOX-mediated oxidative stress in driving steatosis formation. In agreement, incubation with the NOX2/4 inhibitor attenuated or even normalized lipid accumulation and NOX activity (Fig. 7 *F* and *G*) whereas incubation with the NOX4 inhibitor did not reduce superoxide generation (*SI Appendix*, Fig. S5). None of the treatments influenced cell viability.

To further establish the nature and origin of the reactive oxygen species (ROS) measured, we performed a series of additional experiments. NADPH-derived chemiluminescence signal in HepG2 cells was markedly reduced by superoxide dismutase (SOD) whereas incubation with catalase did not influence the signal (*SI Appendix*, Fig. S6), thus demonstrating that this assay is predominantly assessing superoxide generation and not hydrogen peroxide. These results were confirmed also using state-of-the art EPR technology (Fig. 8). Superoxide generation was largely defined to the membrane fraction, which supports NOX as a primary source, rather than cytosolic components such as mitochondria. Steatosis was associated with increased superoxide generation, which was normalized by nitrite treatment (Fig. 8*A*). The 5,5-dimethyl-1-pyrroline *N*-oxide (DMPO)hydroxyl adduct (DMPO-OH) EPR signal from membrane fraction, isolated from HepG2 cells with steatosis, was significantly reduced by the combined NOX2/NOX4 inhibitor GLX481304, and abolished by SOD (Fig. 8 *B* and *C*). Taken together, our data using a lucigenin-chemiluminescence assay and EPR clearly indicate that nitrite attenuates NOX-derived superoxide generation.

Nitrite restores p-AMPK levels and downstream signaling. Like in the in vivo situation, the steatosis-inducing treatment decreased phosphorylated levels of AMPK (Fig. 9*A*) and Akt (*SI Appendix*, Fig. S7) in the HepG2 cells, and, again, nitrite prevented the decline in p-AMPK levels, but not those of p-Akt. For the downstream proteins studied, similar effects as observed in vivo were seen regarding steatosis (*SI Appendix*, Fig. S7). However, the effects of nitrite on these parameters were not as potent as those observed with nitrate in vivo. Next, we tested the effect of compound C, an inhibitor of AMPK, on NOX activity in the steatosis model. Simultaneous incubation with compound C alone did not

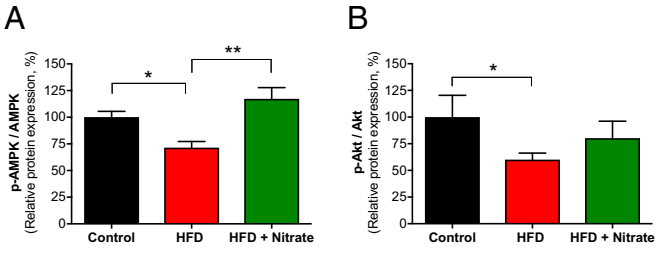

Fig. 5. Liver AMPK and Akt expression. After 7 wk of dietary treatment, mice were killed, and livers from the animals were individually homogenized. The protein levels of p-AMPK/AMPK (*A*) and p-Akt/Akt (*B*) were measured by Western blot, and densitometric quantification is presented as the ratio of p-AMPK/AMPK or p-Akt/Akt. Data are presented as the mean ± SEM. $n = 9$ to 10 (*A* and *B*) per group. * and ** denote $P < 0.05$ and $P < 0.01$, respectively, between indicated groups, tested by Kruskal–Wallis test and Dunn's test. HFD, high-fat diet+L-NAME.

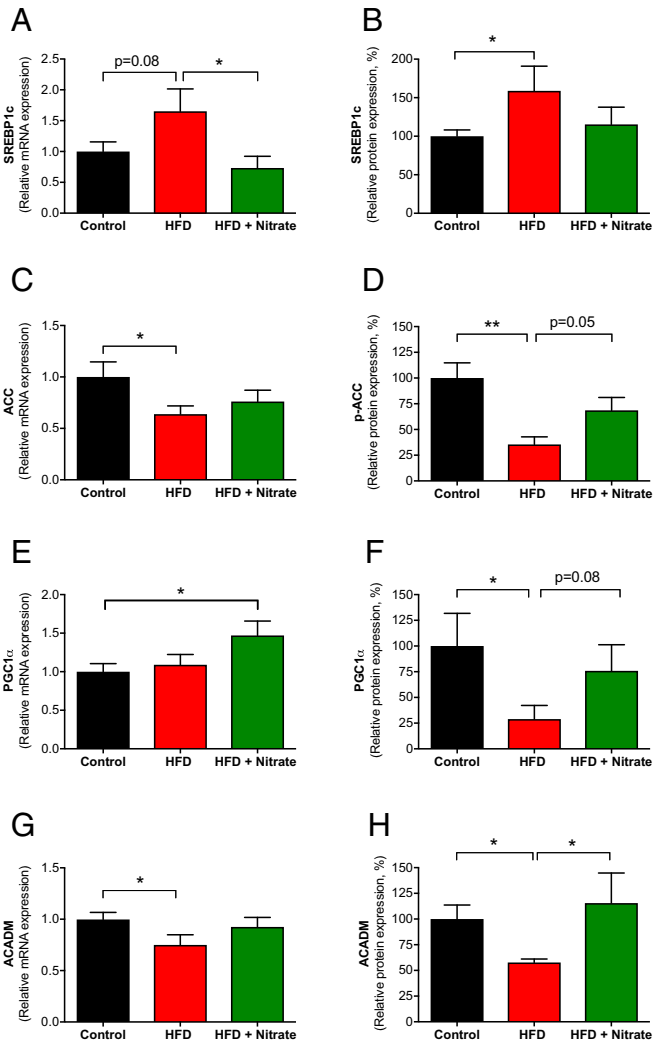

Fig. 6. Expression of metabolic regulatory proteins in the liver. After 7 wk of dietary treatment, mice were killed, and livers from the animals were individually homogenized. The mRNA expression and protein levels of (*A* and *B*) SREBP1c, (*C* and *D*) ACC, (*E* and *F*) PGC1α, and (*G* and *H*) ACADM were measure in the three groups of animals. mRNA expression levels were determined by real-time PCR and protein levels by Western blot. Densitometric quantification is presented as SREBP1c/vinculin, p-ACC/vinculin, PGC1α/vinculin, and ACADM/vinculin. Data are presented as the mean ± SEM. $n = 6$ to 8 (*A*, *C*, *E*, and *G*) and $n = 7$ to 8 (*B*), $n = 8$ to 10 (*D*), $n = 5$ to 6 (*F*), $n = 7$ to 8 (*H*) per group. * and ** denote $P < 0.05$ and $P < 0.01$, respectively, between indicated groups, tested by Kruskal–Wallis test and Dunn's test. ACADM, medium chain acyl-CoA dehydrogenase; ACC, acetyl-CoA carboxylase; HFD, high-fat diet+L-NAME; p-ACC, phospho-ACC; PGC1α, peroxisome proliferator-activated receptor γ coactivator 1 alpha; SREBP1c, transcription factor sterol regulatory element-binding protein 1c.

further increase NOX activity in the cells, but it prevented the salutary effects of nitrite (Fig. 9*B*). Using similar conditions, the NO donor 3,3-Bis(aminoethyl)-1-hydroxy-2-oxo-1-triazene (DETA-NONOate) and the cGMP analog 8-(4-Chlorophenylthio)-guanosine 3′,5′-cyclic monophosphate sodium salt (8-pCPT-cGMP) both restored the p-AMPK/AMPK ratio during steatosis (Fig. 9*C*). Together, these results further support a role of AMPK modulation by NO derived from nitrite and nitrate in prevention of steatosis and oxidative stress.

The protective effects of nitrite involve NO generation and cGMP signaling. In view of these results and to better understand the role of NO and the molecular mechanism(s) of nitrite bioactivation, HepG2 cells were treated with different inhibitors or agonists with or without simultaneous nitrite treatment. Oil Red O staining (Fig. 10*A*) together with NOX activity (Fig. 10*B*) were measured.

Nitrite is a versatile signaling molecule and can exert its biological effects, not only through reduction to NO, but also via the formation of other bioactive nitrogen oxides, including S-nitrosothiols and the nitrogen dioxide radical. However, the favorable effects of nitrite on steatosis and NOX activity were mimicked by the NO donor DETA-NONOate. In addition, the effects of nitrite were abolished in the presence of 1H-[1,2,4]oxadiazolo-[4, 3-a]quinoxalin-1-one (ODQ), an inhibitor of soluble guanylyl cyclase (sGC). Also, the cGMP

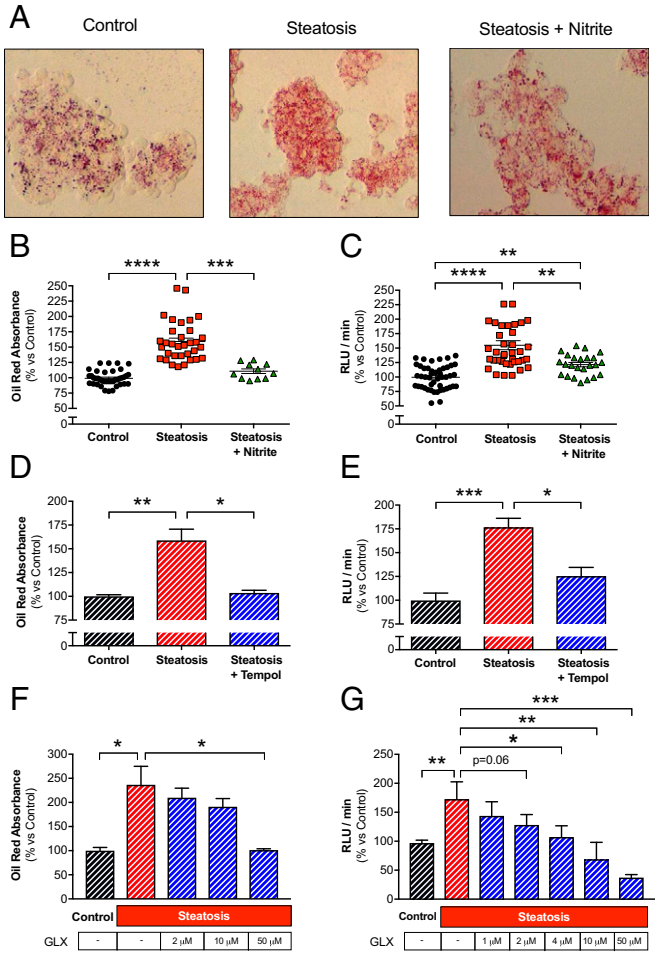

Fig. 7. Oil Red O staining and NADPH oxidase activity in HepG2 cells. Cells were treated with control, steatosis, or steatosis + nitrite media for 24 h. (*A*) Representative images of HepG2 cells from the three groups stained with Oil Red O to visualize neutral lipids. (Magnification: 40×.) (*B*) Semiquantification of neutral lipids in the HepG2 cells measuring absorbance at 520 nm. Each dot represents an individual value. (*C*) NADPH oxidase-derived superoxide production in the HepG2 cells, and expressed as relative light units (RLUs). Each dot represents an individual value. To assess the role of oxidative stress in the development of steatosis, the cells were simultaneously incubated for 24 h with the superoxide scavenger tempol (*D* and *E*) or the NADPH oxidase inhibitor GLX481304 (*F* and *G*). Then, neutral lipids accumulation was measured by Oil Red O (*D* and *F*), and NADPH oxidase-derived superoxide production was measured with a lucigenin-dependent chemiluminescence signal (*E* and *G*). Data are presented as the mean ± SEM. $n = 6$ (*A*), $n = 11$ to 17 (*B*), $n = 26$ to 50 (*C*), $n = 6$ to 8 (*D* and *E*), $n = 4$ to 16 (*F* and *G*) per group. *, **, ***, and **** denote $P < 0.05$, $P < 0.01$, $P < 0.001$, and $P < 0.0001$, respectively, between indicated groups, tested by Kruskal–Wallis test and Dunn's test. Control, 5.5 mM glucose; Steatosis, 25 mM glucose, 10 nM insulin, and 240 μM FFA (steatosis mix); Steatosis + nitrite, steatosis mix + 10 μM sodium nitrite; Steatosis + tempol, steatosis mix + 100 μM tempol; Steatosis + GLX = steatosis mix + 2 to 50 μM GLX481304.

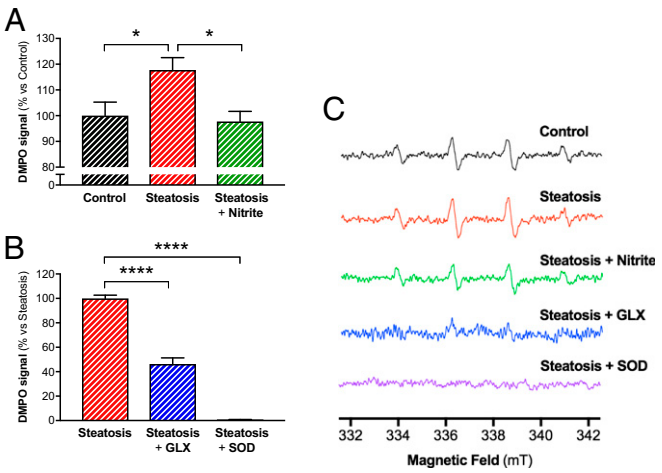

Fig. 8. Assessment of superoxide production in HepG2 cells by EPR. Cells were treated with control, steatosis mixture, or steatosis + nitrite for 48 h. (*A* and *B*) Quantification of second-peak amplitudes of DMPO/•OH adducts from EPR spectra in the membrane fraction of HepG2 cells. Nitrite treatment prevented steatosis-induced increase of $O_2^{\bullet-}$ production (*A*), similar to that achieved with the NOX2/NOX4 inhibitor GLX481304 (*B*). Coincubation with SOD (400 U/mL) completely blunted EPR signals, confirming that DMPO/•OH adducts quantified are from $O_2^{\bullet-}$ (DMPO/•OOH) and not from the hydroxyl (•OH) radical. (*C*) Representative EPR spectrums from *A* and *B* experiments. Data are presented as the mean ± SEM. $n = 4$ to 11 per group. * and **** denote $P < 0.05$ and $P < 0.0001$, respectively, between indicated groups, tested by Kruskal–Wallis test and Dunn's test.

analog 8-pCPT-cGMP was able to mimic the effects of nitrite on steatosis and NOX activity (Fig. 10). The effects of these compounds were mirrored also when looking at activation of AMPK (Fig. 9*C*). To verify that NO was being formed in our systems, we used EPR spin trapping and could confirm NO generation from nitrite-treated HepG2 cells, using ^{14}N nitrite (Fig. 11 *A* and *B*). The use of ^{15}N nitrite (duplet instead of triplet signal) proves that NO is coming from the nitrite added and not an endogenous source (Fig. 11 *C* and *D*). Moreover, nitrite-mediated NO production was significantly attenuated by febuxostat (Fig. 11). However, since NO formation from ^{15}N nitrite was only partially inhibited by febuxostat, other enzymes than XOR must contribute to such an effect. In agreement with nitrite-derived NO formation in the cells, and as described in previous sections, dietary nitrate treatment was associated with increased NO generation, as demonstrated by the restoration of blood Hb-NO and liver DNIC levels in mice fed HFD+L-NAME (Fig. 2 *D* and *E*).

One of the proposed key enzymes involved in the bioactivation of nitrate and nitrite is XOR. Aldehyde oxidase (AO) is another molybdopterin-containing enzyme that may catalyze the one electron reduction of nitrite to NO. We therefore tested the effects of nitrite in the presence of febuxostat, a potent and specific inhibitor of XOR, as well as with an inhibitor of AO (i.e., Raloxifene). Febuxostat did not influence the Oil Red O (ORO) staining (100 ± 9, $n = 6$ vs. 107 ± 5, $n = 6$) or the NOX activity (100 ± 4, $n = 12$ vs. 97 ± 4, $n = 6$), compared with steatosis alone, but blocked the attenuation in NOX activity seen with nitrite treatment (Fig. 10). Moreover, the reduction in lipid accumulation achieved with nitrite exposure was partially lost by XOR inhibition. Similar treatment protocol, but in the presence of Raloxifene, did not significantly influence the degree of lipid accumulation or NOX activity, compared with steatosis, and did not inhibit the favorable effects observed with nitrite (*SI Appendix*, Fig. S8).

Again, in the EPR spin trapping experiments, the nitrite-derived NO signal was attenuated in the presence of febuxostat (Fig. 11). Together, this suggests the involvement of XOR in nitrite bioactivation but also indicates the presence of additional nitrite reductases in HepG2 cells.

Hepatocyte Spheroids (Part III).

Effects of nitrite on steatosis in human liver spheroids. Liver function and pathologies are difficult to study using primary human hepatocyte (PHH) monolayer cultures as they dedifferentiate rapidly, thereby restricting their clinical relevance. We have developed and extensively characterized a 3D PHH spheroid system and have shown that such spheroids remain phenotypically stable, are similar to the liver in vivo, and even retain their interindividual variability from the donor livers (31, 32). Furthermore, the spheroids retain intact morphology, viability, and hepatocyte-specific functions for at least 5 wk. This validated system was used to test the effects of nitrite on the development of steatosis.

Nitrite reverses metabolic-induced steatosis in 3D PHH. When spheroids were exposed to glucose, insulin, and FFA (7 d), clear signs of steatosis developed. We tested if nitrite could affect the reversibility of such metabolic-induced steatosis. After steatosis had developed (7 d), spheroids were treated with nitrite or vehicle, and the recovery was studied 7 d later in the absence of free fatty acids. At this time point the vehicle-treated spheroids still had severe steatosis while nitrite dose-dependently led to recovery (Fig. 12 *A* and *B*). Moreover, incubation with febuxostat abolished the protective effects of nitrite, again indicating a role for XOR in bioactivation of nitrite (Fig. 12*C*). Expression of XOR in the spheroids (3D PHH) was confirmed by proteome analysis (*SI Appendix*, Fig. S9). Similar to that observed in liver tissue from the in vivo model and in HepG2 cells, steatosis was associated with increased NADPH oxidase activity (Fig. 12*D*) and increased expression of its regulatory subunit p67phox (Fig. 12*E*), which were both attenuated by nitrite.

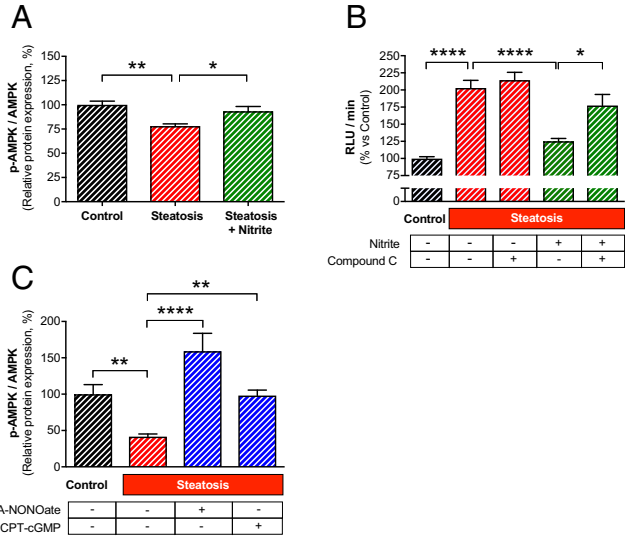

Fig. 9. Regulation of AMPK and NADPH oxidase activity in HepG2 cells. Cells were treated with control, steatosis, or steatosis + nitrite media for 24 h. The protein levels of p-AMPK/AMPK were measured by Western blot. Densitometric quantification is presented as the ratio p-AMPK/AMPK (*A*). Cells were treated with control, steatosis, steatosis + nitrite, steatosis + compound C (an AMPK inhibitor), or steatosis + compound C + nitrite media for 24 h, and NADPH oxidase-derived superoxide formation was measured with lucigenin-dependent chemiluminescence signal in the HepG2 cells, and expressed as relative light units (RLUs) (*B*). Using similar conditions, the effects of an NO donor (DETA-NONOate) and a cGMP analog (8-pCPT-cGMP) on p-AMPK/AMPK ratio were assessed (*C*) during steatosis. Data are presented as the mean ± SEM. $n = 4$ (*A*) and $n = 5$ to 60 (*B*) per group. *, **, and **** denote $P < 0.05$, $P < 0.01$, and $P < 0.0001$, respectively, between indicated groups, tested by Kruskal–Wallis test and Dunn's test. Control, 5.5 mM glucose; Steatosis, 25 mM glucose, 10 nM insulin, and 240 μM FFA (steatosis mix); Steatosis + nitrite, steatosis mix+10 μM sodium nitrite; Steatosis + Compound C, steatosis + 20 μM Compound C; Steatosis + Compound C + nitrite, steatosis mix + 20 μM Compound C + 10 μM sodium nitrite.

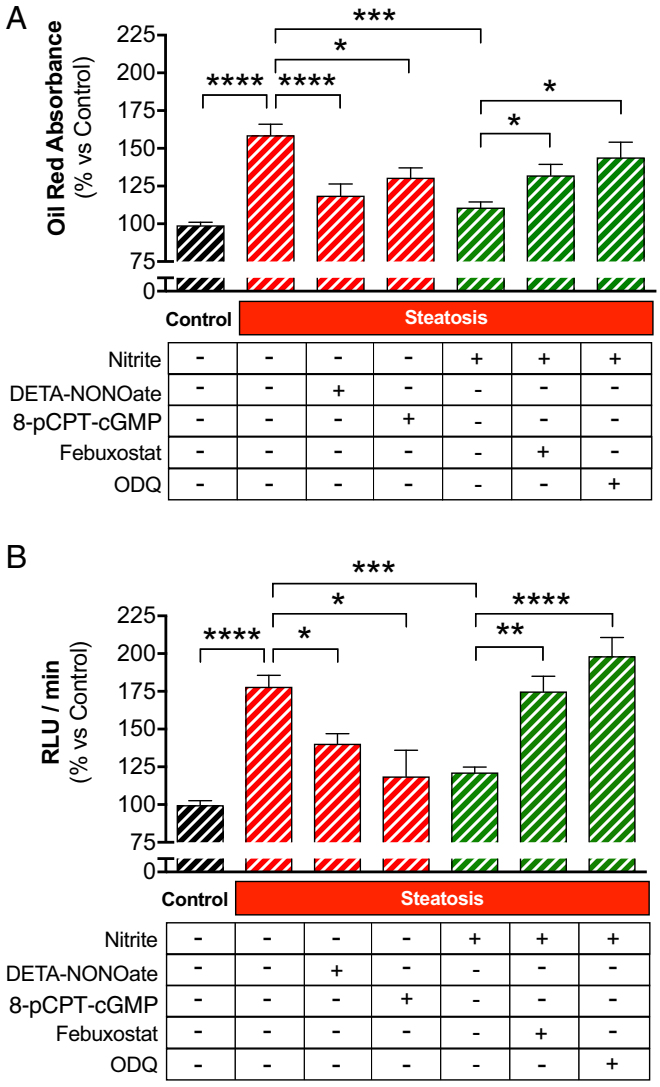

Fig. 10. Mechanisms contributing to nitrite-mediated protection against steatosis in HepG2 cells. Cells were treated with control, steatosis, steatosis + nitrite, steatosis + DETA-NONOate (a slow releasing NO-donor), steatosis + cGMP analog (8-pCPT-cGMP), steatosis + Febuxostat (a specific inhibitor of XOR), or steatosis + ODQ (an inhibitor of soluble guanylyl cyclase) media for 24 h. (*A*) Accumulation of neutral lipids was measured by Oil Red O, and (*B*) NADPH oxidase-derived superoxide formation was measured with lucigenin-dependent chemiluminescence signal, and expressed as relative light units (RLUs). Data are presented as the mean ± SEM. $n = 5$ to 32 (*A*) and $n = 5$ to 60 (*B*) per group. *, **, ***, and **** denote $P < 0.05$, $P < 0.01$, $P < 0.001$, and $P < 0.0001$, respectively, between indicated groups, tested by Kruskal–Wallis test and Dunn's test. Control, 5.5 mM glucose; Steatosis, 25 mM glucose, 10 nM insulin, and 240 μM FFA (steatosis mix); Steatosis + nitrite, steatosis mix + 10 μM sodium nitrite; Steatosis + DETA-NONOate, steatosis mix+ 5 μM DETA-NONOate; Steatosis + cGMP analog, steatosis mix + 10 μM cGMP analog; Steatosis + Febuxostat, steatosis mix + 50 nM Febuxostat; Steatosis + ODQ, steatosis mix + 10 μM ODQ.

Nitrite attenuates drug-induced steatosis in 3D PHH. Next, we tested if simultaneous incubation with nitrite could attenuate drug-induced steatosis. When spheroids were exposed to the hepatotoxic drug amiodarone (14 d), clear signs of steatosis had developed (Fig. 13). Coincubation with nitrite clearly prevented lipid accumulation. Remarkably, these favorable effects of nitrite on metabolic- and drug-induced steatosis were significant already at 1 μM, which is similar to the levels of endogenous nitrite found in healthy tissues under basal conditions.

Discussion

Here, we show that dietary inorganic nitrate preserves metabolic and cardiovascular function and markedly attenuates liver steatosis in mice with diet-induced metabolic syndrome. The favorable effects of nitrate on development of steatosis occurred despite similar accumulation of fat mass. These salutary effects were reflected in experiments using HepG2 cells and in 3D spheroids from primary human liver cells. Dietary nitrate in vivo and nitrite in vitro activated AMPK and reduced NOX activity, leading to enhanced NO bioavailability and cardiometabolic improvement.

Dietary nitrate is metabolized in vivo to first form the more reactive nitrite anion (12). It has been suggested that oral bacteria have a key role in nitrate bioactivation, but mammalian systems have also been demonstrated (33). Our data from normal and germ-free mice indicate a central role of bacteria in nitrate bioactivation. Thus, the protective effects of nitrate on development of liver steatosis were absent in germ-free animals. Because the nitrate ion in itself is more or less biologically inert, we later used nitrite in all subsequent in vitro experiments. When human liver spheroids were exposed to nitrite, the degree of steatosis induced by either nutritional overload or amiodarone was significantly decreased. Remarkably, the effects of nitrite in vitro were seen already at submicromolar levels: i.e., close to what is seen in tissues under basal conditions and definitely what is achieved after ingestion of nitrate-rich vegetables (12, 17).

Mechanistically, the effects of nitrite seemed to be mediated by its reduction to NO and a further cGMP-mediated activation of AMPK, a master regulator of cellular metabolism and energy homeostasis. Formation of NO from nitrate in vivo was verified with EPR methodology detecting two specific NO-derived species in blood and liver tissue and from nitrite in cells using a spin trap. The reduction of nitrate to NO-species in vivo was confirmed by an EPR method detecting Hb-NO in whole blood and DNICs in liver. Additionally, the NO (^{15}N) formation from nitrite (^{15}N) in cultured cells was demonstrated by EPR spin trapping using Fe(II)-diethyldithiocarbamate colloid (Fe-DETC) (34). Recent studies

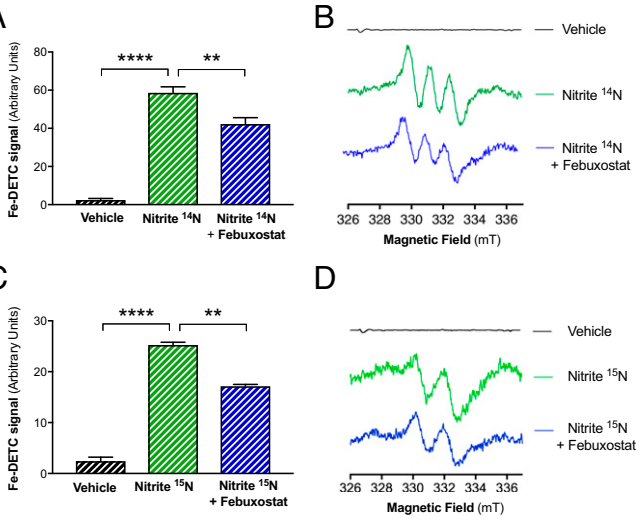

Fig. 11. Affirmation of nitrite-mediated NO production in HepG2 cells by EPR. Changes in first-peak amplitudes from EPR spectrums, together with representative spectrums, for NO production using $Fe(DETC)_2$ as spin trap. HepG2 cells were incubated with vehicle or Febuxostat (50 nM) for 20 min and then treated with nitrite ^{14}N (500 μM) or nitrite ^{15}N (500 μM) for 1 h in the presence of 0.5 mM colloid $Fe(DETC)_2$ for NO detection. Shown are quantified EPR data for nitrite ^{14}N (*A* and *B*) and nitrite ^{15}N (*C* and *D*) together with representative spectrums for the different experiments. Data are presented as the mean ± SEM. $n = 3$ to 4 per group. ** and **** denote $P < 0.01$ and $P < 0.0001$, respectively, between indicated groups, tested by Kruskal–Wallis test and Dunn's test.

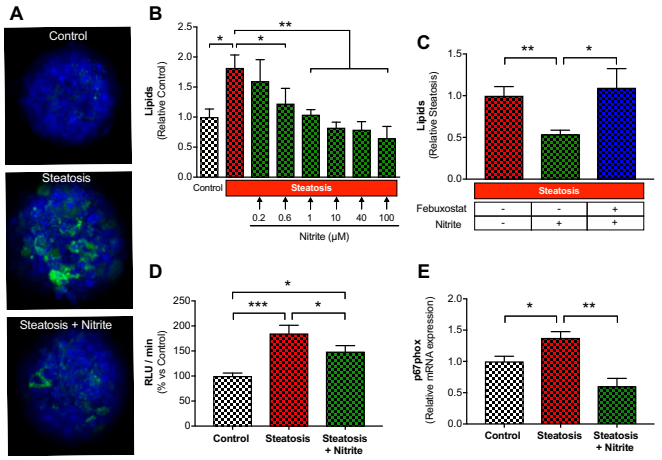

Fig. 12. Reversibility of metabolic steatosis in primary human hepatocyte spheroids. Spheroids were exposed to higher concentration of FFA (320 μM) in the medium for 1 wk to induce steatosis. Thereafter, the metabolic steatotic stimuli were removed, and the spheroids were treated with or without increasing concentrations of nitrite (0.2 to 100 μM) for 7 d. The spheroids were stained, and the degree of steatosis (i.e., lipid content) was evaluated by the AdipoRed fluorescence technique. Nitrite improved reversibility of metabolic-induced steatosis in a dose-dependent way (*A* and *B*), being significant compared with the steatosis group at concentrations ≥0.6 μM. Representative images are shown for the three groups (nitrite, 10 μM) (staining with Nile Red staining) (*A*). Simultaneous treatment with febuxostat completely inhibited the favorable effects of nitrite on lipid accumulation (*C*). Similar to that observed in vivo and in HepG2 cells, steatosis was associated with increased NADPH oxidase activity, measured as changes in relative light units (RLUs) (*D*) and increased expression of its regulatory subunit p67phox (*E*), which were both attenuated by nitrite (10 μM) treatment. Data are presented as the mean ± SEM. $n = 6$ to 16 (*B*), $n = 8$ to 12 (*C*), $n = 8$ (*D*), $n = 3$ to 5 (*E*) per group. All data were obtained from one donor. *, **, and *** denote $P < 0.05$, $P < 0.01$, and $P < 0.001$, respectively, between indicated groups. Tests performed by one-way ANOVA followed by Holm–Sidak test. (Magnification: 10×.)

suggest a new role for mobile iron-nitrosylated-Hb complexes (heme-NO and DNICs), as signaling species, additionally (or alternatively) to free NO (35, 36). It would be worthwhile to conduct studies to verify if iron-nitrosylated-Hb species play a role in the metabolic effects of dietary nitrate.

The protective effects of nitrite were mimicked by an NO donor and a cGMP analog and blocked by ODQ, an inhibitor of guanylyl cyclase. These results are in line with those of Deshmukh et al. (37), who described an insulin-independent activation of AMPK by cGMP. Nitrate and nitrite also decreased liver NOX activity both in vivo and in vitro. The degree of inhibition by dietary nitrate correlated to the improvement of steatosis, indicating that this inhibition is central to the salutary effects observed. A role for oxidative stress is further supported by the inhibitory effects of the superoxide scavenger tempol and the NOX inhibitor GLX481304 on steatosis development in the cell studies. With less superoxide generated, more NO will survive to enhance cGMP-mediated AMPK activation. Additionally, any ROS-mediated direct repression of AMPK phosphorylation (38) is attenuated by the NOX inhibition, creating somewhat of a virtuous cycle. These proposed mechanisms for nitrate-induced liver protection are illustrated in Fig. 14.

XOR has emerged as an important nitrite reductase mediating many of the cardiovascular effects of nitrate and nitrite seen in animal models (15, 39). Up-regulation of XOR is seen in eNOS-deficient mice (40) and in germ-free mice (41), which display abrogated NO and nitrite generation, respectively. This suggests the existence of a system striving to ensure intact overall NO homeostasis. It has remained unclear if XOR-mediated nitrite reduction is of any significance in humans as its expression is so much more prominent in rodents. Here, we establish a role of XOR in nitrite-mediated protection against steatosis in a human cell line and in primary human liver 3D spheroids. There was a significant inhibition of the nitrite effects in the presence of febuxostat although, in the HepG2 cells, the blockade was not complete, thus clearly indicating the presence of other nitrite-reducing systems. Indeed, a number of other nitrite reductases have been described, including mitochondrial proteins and enzymes in the cytochrome P450 family (42).

NAFLD is extremely common and represents a major risk factor for development of more serious liver disease, including steatohepatitis, fibrosis, and cirrhosis. A number of large clinical trials designed to identify effective treatments for nonalcoholic steatohepatitis are in progress, but, as of today, no agent has yet received approval by the Food and Drug Administration. It remains to be studied if dietary intervention with a high intake of nitrate-rich vegetables or a nitrate salt would be of clinical value to treat or prevent fatty liver disease in humans. Nevertheless, it is intriguing that previous epidemiological studies have pinpointed green leafy vegetables—the dominating dietary source of nitrate—as protective against cardiovascular and metabolic disease and T2D (43–45).

Dietary nitrate also had protective effects on the cardiovascular dysfunction that developed as a result of the HFD and chronic inhibition of NOS. Remarkably, blood pressure was essentially normalized with nitrate, and endothelial function was partly preserved, as shown in the ex vivo vascular relaxation studies. The addition of NOS inhibition to this model was included to ensure and augment a metabolic syndrome-like phenotype in the in vivo

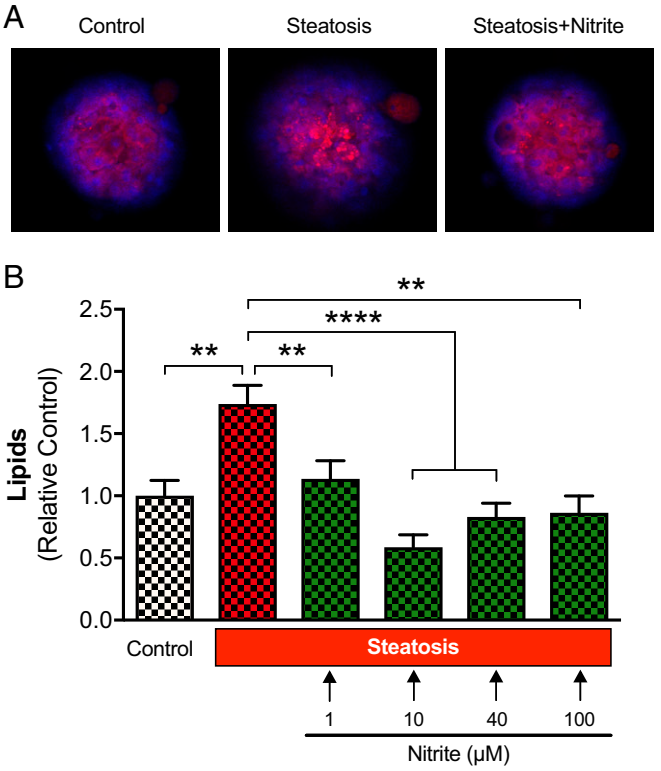

Fig. 13. Drug-induced steatosis in primary human hepatocyte spheroids. Spheroids were exposed to amiodarone (5 μM) in the medium for 14 d to induce steatosis with or without increasing concentrations of nitrite (1 to 100 μM). The spheroids were stained, and the degree of steatosis (i.e., lipid content) was evaluated by the AdipoRed fluorescence technique. Nitrite significantly improved drug-induced steatosis (*A* and *B*) at concentrations ≥1 μM. Representative images are shown for the three groups (nitrite, 10 μM) (*A*). Data are presented as the mean ± SEM. $n = 8$ to 20 per group. ** and **** denote $P < 0.01$ and $P < 0.0001$, respectively, between indicated groups. Tests were performed by one-way ANOVA followed by Holm–Sidak test. (Magnification: 10×.)

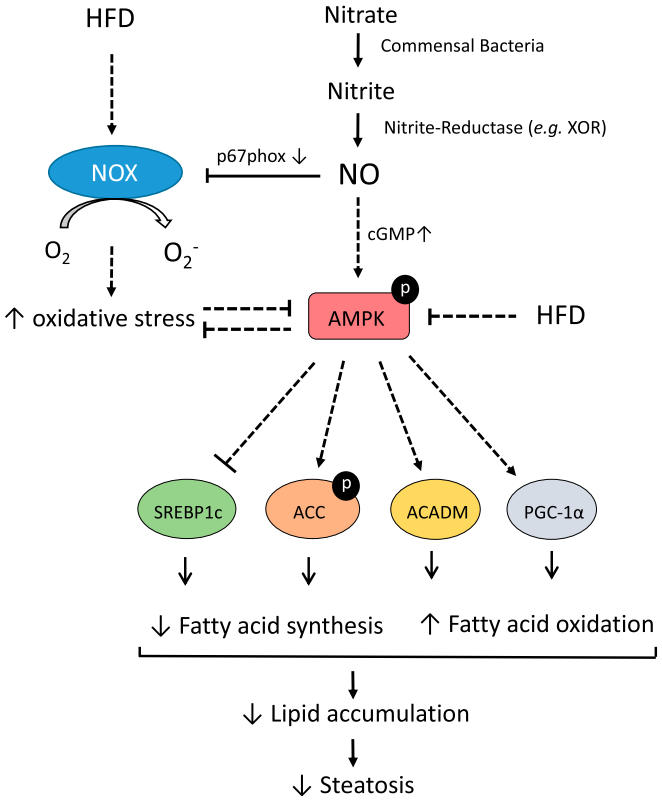

Fig. 14. Metabolic signaling pathways in the liver affected by dietary nitrate. Shown is a simplified scheme illustrating some of the key pathways affected by dietary nitrate to attenuate diet-induced liver steatosis. A high-fat diet (HFD) leads to down-regulation of AMPK activity in at least two ways. First, the surplus of energy will down-regulate AMPK via direct mechanisms involving changes in cellular energy status (AMP/ADP to ATP ratio). Moreover, an HFD leads to activation of NADPH oxidase (NOX) activity, and the resulting oxidative stress can inhibit AMPK activation. Dietary nitrate can counteract this process via formation of nitrite, nitric oxide (NO), and other bioactive nitrogen oxide species. Bioactivation of nitrate depends on commensal bacteria and nitrite reductase activity [e.g., xanthine oxidoreductase (XOR)], respectively. NO serves to down-regulate NOX activity, at least in part via reduction of p67phox expression, and can also activate AMPK in a cGMP-dependent way. The reversal of the HFD-induced AMPK depression by nitrate ultimately affects a number of downstream pathways (i.e., inhibition of SREBP1c, stimulation of ACC phosphorylation, and by restoration of ACADM and PGC1α) to reduce lipid accumulation and steatosis.

studies (Fig. 1). With this combination, one cannot exactly judge the relative contribution of the HFD vs. the L-NAME treatment to the overall phenotype, and it also makes conclusions about the exact mechanisms more complicated. However, one should note that a similar cardiometabolic protection was seen also in additional experiments without systemic NOS inhibition and that L-NAME was not a part of any of the subsequent cell studies. So, clearly, all pathways affected by nitrate/nitrite were so also in the presence of a functional NOS. Moreover, the favorable effects of nitrate on liver steatosis appear to be independent of changes in body weight or accumulation of visceral adipose tissue as protection was observed in both mice fed with HFD+L-NAME (i.e., no effect of nitrate on body weight and fat content) and HFD alone (i.e., body weight and fat content were reduced by nitrate).

We conclude that dietary nitrate attenuates oxidative stress and preserves liver AMPK activity in a mouse model of cardiometabolic dysfunction, with salutary effects on cardiovascular and metabolic function. These effects seemed to be mediated by bacteria-dependent formation of nitrite followed by XOR-dependent reduction of nitrite to NO and generation of cGMP. Moreover, nitrate and nitrite potently protected against diet-induced liver steatosis in vivo, as well as in a human cell line and in spheroids from primary human liver cells. It would be worthwhile to conduct clinical trials to elucidate if dietary nitrate supplementation could be useful in prevention and treatment of T2D and its complications.

Methods

This study was approved by the regional Institutional Animal Care and Use Committee and performed according to the National Institutes of Health guidelines and with the European Union (EU) Directive 2010/63/EU for the conduct of experiments in animals. An overview of the experimental protocol is shown in *SI Appendix*, Fig. S1. Details about the experimental approaches and the cellular, molecular, and biochemical analyses may be found in *SI Appendix, SI Methods*.

In Vivo Mouse Model (Part I). Male C57BL/6J mice (12 wk old; Janvier Labs) were fed with an HFD or HFD+L-NAME for 7 wk, with or without simultaneous supplementation with inorganic nitrate in the drinking water (1.0 mmol·kg^{-1}·d^{-1}). Cardiovascular and metabolic functions were continuously monitored, and, after 7 wk of treatment, the animals were killed, and tissues of interest were collected for analyses (*SI Appendix, SI Methods*). In a separate series of experiments, germ-free mice were used to investigate the role of bacteria in the bioactivation of inorganic nitrate.

HepG2 Cells (Part II). Human HepG2 cells were incubated with a mixture of high glucose, insulin, and FFA to induce steatosis. The effects of simultaneous treatment with inorganic nitrite (10 μM) on steatosis and underlying mechanisms were investigated.

Primary Human Hepatocyte Spheroids (Part III). A 3D model of primary human hepatocyte (PHH) was used, as described previously (31). In short, cryopreserved PHHs were used for formation of spheroid cultures. Hepatic steatosis was induced with a combination of palmitic and oleic acid (metabolic-induced steatosis) or by using amiodarone (pharmacologic-induced steatosis). The AdipoRed Adipogenesis Assay was used to evaluate the degree of steatosis. The effects of inorganic nitrite in different concentrations (0.2 to 100 μM) on steatosis and underlying mechanisms were investigated.

Statistics. Data are presented as the mean ± SEM unless otherwise indicated. Statistical analysis was performed by using one-way, two-way ANOVA or nonparametric Kruskal–Wallis test, followed by post hoc test for comparisons among the groups. A P value of less than 0.05 was considered statistically significant. All statistical analysis was performed using GraphPad Prism, version 7 (GraphPad Software).

ACKNOWLEDGMENTS. We thank Freiberg Instruments Ltd for the use of their EPR equipment (Magnettech MiniScope MS5000). We thank Glucox Biotech AB Stockholm for the kind gift of their NADPH oxidase inhibitors (GLX481304 and GLX7013114). We thank Carina Nihlén, Annika Olsson, Margareta Stensdotter, and Inger Johansson (Karolinska Institutet) for technical assistance. I.C.-H. is supported by a Novo Nordisk postdoctoral fellowship run in partnership with the Karolinska Institutet. This work was supported by Swedish Research Council Grants 2015-02760 and 2016-01381, by Swedish Heart and Lung Foundation Grants 20140448 and 20170124, by Novo-Nordisk Grant 2-4078/2014, by European Research Council Advanced Grant (ERC-AdG) Project HEPASPHER Grant Agreement 742020, and by research funds (2-560/2015) and internal Karolinska Institutet funding for doctoral education (KID) (2-3707/2013 and 2-1930/2016). M.K. was funded by an MD PhD program [Clinical Scientist Training Programme (CSTP)] grant from the Karolinska Institutet. The confocal microscope used was obtained by funding from the Knut and Alice Wallenberg Foundation (Grant KAW2008.0149).

1. Diehl AM, Day C (2017) Cause, pathogenesis, and treatment of nonalcoholic steatohepatitis. *N Engl J Med* 377:2063–2072.
2. Després JP, Lemieux I (2006) Abdominal obesity and metabolic syndrome. *Nature* 444:881–887.
3. Després JP, et al. (2008) Abdominal obesity and the metabolic syndrome: Contribution to global cardiometabolic risk. *Arterioscler Thromb Vasc Biol* 28:1039–1049.
4. Lundberg JO, Gladwin MT, Weitzberg E (2015) Strategies to increase nitric oxide signalling in cardiovascular disease. *Nat Rev Drug Discov* 14:623–641.
5. Litvinova L, et al. (2015) Nitric oxide and mitochondria in metabolic syndrome. *Front Physiol* 6:20.
6. Monti LD, et al. (2003) Endothelial nitric oxide synthase polymorphisms are associated with type 2 diabetes and the insulin resistance syndrome. *Diabetes* 52:1270–1275.
7. Fernandez ML, et al. (2004) Association of NOS3 gene with metabolic syndrome in hypertensive patients. *Thromb Haemost* 92:413–418.

8. Bressler J, Pankow JS, Coresh J, Boerwinkle E (2013) Interaction between the NOS3 gene and obesity as a determinant of risk of type 2 diabetes: The atherosclerosis risk in communities study. *PLoS One* 8:e79466.
9. Cook S, et al. (2003) Clustering of cardiovascular risk factors mimicking the human metabolic syndrome X in eNOS null mice. *Swiss Med Wkly* 133:360–363.
10. Huang PL (2009) eNOS, metabolic syndrome and cardiovascular disease. *Trends Endocrinol Metab* 20:295–302.
11. Carlström M, et al. (2010) Dietary inorganic nitrate reverses features of metabolic syndrome in endothelial nitric oxide synthase-deficient mice. *Proc Natl Acad Sci USA* 107:17716–17720.
12. Lundberg JO, Weitzberg E, Gladwin MT (2008) The nitrate-nitrite-nitric oxide pathway in physiology and therapeutics. *Nat Rev Drug Discov* 7:156–167.
13. Lundberg JO, Govoni M (2004) Inorganic nitrate is a possible source for systemic generation of nitric oxide. *Free Radic Biol Med* 37:395–400.
14. Helms CC, Liu X, Kim-Shapiro DB (December 21, 2016) Recent insights into nitrite signaling processes in blood. *Biol Chem*, 10.1515/hsz-2016-0263.
15. Cantu-Medellin N, Kelley EE (2013) Xanthine oxidoreductase-catalyzed reduction of nitrite to nitric oxide: Insights regarding where, when and how. *Nitric Oxide* 34:19–26.
16. Lundberg JO, et al. (2009) Nitrate and nitrite in biology, nutrition and therapeutics. *Nat Chem Biol* 5:865–869.
17. Lundberg JO, Carlström M, Larsen FJ, Weitzberg E (2011) Roles of dietary inorganic nitrate in cardiovascular health and disease. *Cardiovasc Res* 89:525–532.
18. Hezel M, et al. (2016) Dietary nitrate improves age-related hypertension and metabolic abnormalities in rats via modulation of angiotensin II receptor signaling and inhibition of superoxide generation. *Free Radic Biol Med* 99:87–98.
19. Peleli M, et al. (2015) In adenosine A2B knockouts acute treatment with inorganic nitrate improves glucose disposal, oxidative stress, and AMPK signaling in the liver. *Front Physiol* 6:222.
20. Nyström T, et al. (2012) Inorganic nitrite stimulates pancreatic islet blood flow and insulin secretion. *Free Radic Biol Med* 53:1017–1023.
21. Larsen FJ, et al. (2011) Dietary inorganic nitrate improves mitochondrial efficiency in humans. *Cell Metab* 13:149–159.
22. Gao X, et al. (2015) NADPH oxidase in the renal microvasculature is a primary target for blood pressure-lowering effects by inorganic nitrate and nitrite. *Hypertension* 65: 161–170.
23. Montenegro MF, et al. (2011) Sodium nitrite downregulates vascular NADPH oxidase and exerts antihypertensive effects in hypertension. *Free Radic Biol Med* 51:144–152.
24. Yang T, et al. (2017) Dietary nitrate attenuates renal ischemia-reperfusion injuries by modulation of immune responses and reduction of oxidative stress. *Redox Biol* 13: 320–330.
25. Yang T, et al. (2015) Inorganic nitrite attenuates NADPH oxidase-derived superoxide generation in activated macrophages via a nitric oxide-dependent mechanism. *Free Radic Biol Med* 83:159–166.
26. Appel LJ, et al.; DASH Collaborative Research Group (1997) A clinical trial of the effects of dietary patterns on blood pressure. *N Engl J Med* 336:1117–1124.
27. Liese AD, Nichols M, Sun X, D'Agostino RB, Jr, Haffner SM (2009) Adherence to the DASH diet is inversely associated with incidence of type 2 diabetes: The insulin resistance atherosclerosis study. *Diabetes Care* 32:1434–1436.
28. Ahluwalia A, et al. (2016) Dietary nitrate and the epidemiology of cardiovascular disease: Report from a National Heart, Lung, and Blood Institute Workshop. *J Am Heart Assoc* 5:e003402.
29. Ghasemi A, Jeddi S (2017) Anti-obesity and anti-diabetic effects of nitrate and nitrite. *Nitric Oxide* 70:9–24.
30. Winerdal M, et al. (2017) Single dose caffeine protects the neonatal mouse brain against hypoxia ischemia. *PLoS One* 12:e0170545.
31. Bell CC, et al. (2016) Characterization of primary human hepatocyte spheroids as a model system for drug-induced liver injury, liver function and disease. *Sci Rep* 6: 25187.
32. Kozyra M, et al. (2018) Human hepatic 3D spheroids as a model for steatosis and insulin resistance. *Sci Rep* 8:14297.
33. Jansson EA, et al. (2008) A mammalian functional nitrate reductase that regulates nitrite and nitric oxide homeostasis. *Nat Chem Biol* 4:411–417.
34. Kleschyov AL, et al. (2000) Spin trapping of vascular nitric oxide using colloid Fe(II)-diethyldithiocarbamate. *Biochem Biophys Res Commun* 275:672–677.
35. Vanin AF (2016) Dinitrosyl iron complexes with thiol-containing ligands as a "working form" of endogenous nitric oxide. *Nitric Oxide* 54:15–29.
36. Kleschyov AL (2017) The NO-heme signaling hypothesis. *Free Radic Biol Med* 112: 544–552.
37. Deshmukh AS, et al. (2010) Nitric oxide increases cyclic GMP levels, AMP-activated protein kinase (AMPK)alpha1-specific activity and glucose transport in human skeletal muscle. *Diabetologia* 53:1142–1150.
38. Ruderman NB, Carling D, Prentki M, Cacicedo JM (2013) AMPK, insulin resistance, and the metabolic syndrome. *J Clin Invest* 123:2764–2772.
39. Khambata RS, Ghosh SM, Ahluwalia A (2015) "Repurposing" of xanthine oxidoreductase as a nitrite reductase: A new paradigm for therapeutic targeting in hypertension. *Antioxid Redox Signal* 23:340–353.
40. Peleli M, et al. (2016) Enhanced XOR activity in eNOS-deficient mice: Effects on the nitrate-nitrite-NO pathway and ROS homeostasis. *Free Radic Biol Med* 99:472–484.
41. Huang L, Borniquel S, Lundberg JO (2010) Enhanced xanthine oxidoreductase expression and tissue nitrate reduction in germ free mice. *Nitric Oxide* 22:191–195.
42. van Faassen EE, et al. (2009) Nitrite as regulator of hypoxic signaling in mammalian physiology. *Med Res Rev* 29:683–741.
43. Bazzano LA, Li TY, Joshipura KJ, Hu FB (2008) Intake of fruit, vegetables, and fruit juices and risk of diabetes in women. *Diabetes Care* 31:1311–1317.
44. Carter P, Gray LJ, Troughton J, Khunti K, Davies MJ (2010) Fruit and vegetable intake and incidence of type 2 diabetes mellitus: Systematic review and meta-analysis. *BMJ* 341:c4229.
45. Bondonno CP, et al. (2017) Association of vegetable nitrate intake with carotid atherosclerosis and ischemic cerebrovascular disease in older women. *Stroke* 48: 1724–1729.